

**Mass and radius determination for the neutron star in X-ray burst source 4U/MXB 1728-34**

by

A. Majczyna and J. Madej

Warsaw University Observatory, Al. Ujazdowskie 4, 00-478 Warsaw, Poland  
email: jm@astrouw.edu.pl**Abstract**

We analyzed archival X-ray spectra of MXB 1728-34 obtained in 1996-99 by the Proportional Counter Array on board of the RXTE satellite. X-ray spectra were fitted to our extensive grids of model atmosphere spectra to determine the effective temperature  $T_{\text{eff}}$  on the neutron star surface, logarithm of surface gravity  $\log g$ , and the gravitational redshift  $z$  simultaneously. We have chosen fitting by numerical model spectra plus broad Gaussian line, modified by interstellar absorption and the absorption on dust. We arbitrarily assumed either hydrogen-helium chemical composition of a model atmosphere, or H-He-Fe mixture in solar proportion. The statistically best values of  $\log g$ , and  $z$  subsequently were used to determine mass and radius of the neutron star. We obtained the best values of the parameters for the neutron star in X-ray burst source MXB 1728-34: mass either  $M = 0.40$  or  $0.63M_{\odot}$  (for H-He or H-He-Fe models, respectively), radius  $R = 4.6$  or  $5.3$  km,  $\log g = 14.6$  or  $14.6$  and the gravitational redshift  $z = 0.14$  or  $0.22$ . All the above parameters have very wide  $1-\sigma$  confidence limits. Their values strongly support the equation of state for strange matter in MXB 1728-34.

**Key words** *Stars: fundamental parameters – stars: neutron – X-rays: bursts – stars: individual (MXB 1728-34)*

**1. Introduction**

X-ray source MXB 1728-34 was discovered in 1976 by Forman, Tananbaum & Jones (1976) in the survey observations of the Uhuru satellite. Type I X-ray bursts from this source were identified in the same year by Lewin, Clark & Doty (1976) in SAS-3 satellite data. Optical counterpart still remains unidentified probably due to large extinction in the direction to this source. Recently Martí et al. (1998) has identified an infrared counterpart to MXB 1728-34, but the connection with the X-ray source has not yet been confirmed. MXB 1728-34 was observed in a wide energy range from radio (Martí et al. 1998) to  $\gamma$ -ray energies (cf. Claret et al. 1994).

The determination of mass and radius of a neutron stars is a very important and interesting problem, because it allows one to determine or to constrain the equation

of state of superdense matter. Distance to the source is also necessary to localize the source relatively to the Galactic center. For MXB 1728-34 the first estimate of its distance  $d$  and true radius  $R$  was given by van Paradijs (1978),  $d = 4.2 \pm 0.2$  kpc and  $R = 6.5 \pm 0.4$  km (see also Foster et al. 1986). Both parameters were estimated assuming that the peak flux of a given burst from this source approached the Eddington limiting flux. It became immediately clear that such a radius  $R$  was smaller than the minimum radius expected for a neutron star of the canonical mass of  $1.4M_{\odot}$ .

MXB 1728-34 was frequently observed in X-rays after that year, and parameters of the neutron star were estimated in several papers. Kaminker et al. (1989) interpreted spectra of this source using simplified emission models. They have derived the following values of the neutron star parameters: mass  $M = 1.4 - 2.0M_{\odot}$  and radius  $R = 6.5 - 12$  km assuming the distance  $d = 6$  kpc and pure helium atmosphere.

Di Salvo et al. (2000) and Galloway et al. (2003) also assumed, that luminous bursts from this source are standard candles of the bolometric luminosity at the Eddington limit. They concluded that the distance to this X-ray burster is in the range  $4.4 - 5.1$  kpc.

On the other hand, Shaposhnikov et al. (2003) obtained other values:  $d = 4.5 - 5.0$  kpc,  $M = 1.2 - 1.6M_{\odot}$ , and  $R = 8.7 - 9.7$  km. They also concluded, that the helium mass abundance  $Y > 0.9$  in atmosphere of the neutron star in MXB 1728-34. These authors used semianalytical models of expanding atmospheres by Titarchuk (1994), and Titarchuk & Shaposhnikov (2002).

A different approach to this problem was used by Li et al. (1999), who interpreted power spectra of the X-ray light curve and compared them to the model by Osherovich & Titarchuk (1999) and Titarchuk & Osherovich (1999). As the result Li et al. (1999) constrained the area on the  $(M, R)$  plane, where the neutron star of MXB 1728-34 is located. Constrained localization of MXB 1728-34 was characteristic for a star built up of strange matter.

We present here for the first time the estimation of mass and radius of MXB 1728-34, obtained by fitting of archival RXTE X-ray spectra of this source to the new extensive grids of model atmospheres and theoretical spectra of neutron stars. This technique also allowed us to obtain the upper limit of the distance to MXB 1728-34. Theoretical model spectra were obtained with the ATM21 code, which computes model atmospheres of hot neutron stars with the account of Compton scattering on free electrons. The code takes into account angle-averaged Compton scattering of X-ray photons with initial energies approaching the electron rest mass.

Detailed description of the equations and numerical methods were given in a long series of earlier papers (Madej 1991a,b; Joss & Madej 2001; Majczyna et al. 2002; Madej, Joss & Różańska 2004; Majczyna et al. 2005).

## 2. Model atmospheres and theoretical spectra

Model atmospheres used in this paper are based on the equation of radiative transfer of the following form

$$\begin{aligned} \mu \frac{\partial I_{\nu}(z, \mu)}{\rho \partial z} &= \kappa'_{\nu} (1 - e^{-h\nu/kT}) (B_{\nu} - I_{\nu}) \\ &+ \left(1 + \frac{c^2}{2h\nu^3} I_{\nu}\right) \oint_{\omega'} \frac{d\omega'}{4\pi} \int_0^{\infty} \frac{\nu}{\nu'} \sigma(\nu' \rightarrow \nu, \vec{n}' \cdot \vec{n}) I_{\nu'}(z, \vec{n}') d\nu' \\ &- I_{\nu}(z, \mu) \oint_{\omega'} \frac{d\omega'}{4\pi} \int_0^{\infty} \sigma(\nu \rightarrow \nu', \vec{n} \cdot \vec{n}') \left(1 + \frac{c^2}{2h\nu'^3} I_{\nu'}\right) d\nu', \end{aligned} \quad (1)$$

which defines a very elaborate source function  $S_{\nu}$  of our models (Madej 1991a). The significance of symbols in Eq. 1 is commonly known and will not be repeated here.

We stress here, that our theoretical models use sophisticated Compton scattering cross-sections  $\sigma(\nu \rightarrow \nu', \vec{n} \cdot \vec{n}')$ , which allow for a large photon energy change at the time of a single scattering off electrons with a relativistic thermal velocity distribution (Guilbert 1981). Frequently used Kompaneets approximation was rejected in our calculations in order to obtain high numerical accuracy of theoretical Comptonised X-ray spectra.

The actual code is able to compute model atmospheres and theoretical X-rays spectra of very hot neutron stars, taking also into account numerous bound-free and free-free monochromatic opacities of various elements, and the equation of state of ideal gas. The code is “exact” in that it solves the equation of transfer coupled with the equation of radiative equilibrium using partial linearisation and variable Eddington factors technique (Mihalas 1978).

We calculated 3 extensive grids of model atmospheres of hot neutron stars corresponding to various arbitrarily assumed chemical compositions.

- Hydrogen-helium mixture with solar helium number abundance,  $N_{He}/N_H = 0.11$  (223 models),
- Hydrogen-helium-iron mixture with  $N_{He}/N_H = 0.11$  and solar iron number abundance,  $N_{Fe}/N_H = 3.7 \times 10^{-5}$  (228 models),
- Hydrogen-helium-iron mixture with  $N_{He}/N_H = 0.11$  and  $100 \times$  solar iron number abundance,  $N_{Fe}/N_H = 3.7 \times 10^{-3}$  (229 models).

Computed models cover the range of  $1 \times 10^7 \leq T_{\text{eff}} \leq 3 \times 10^7$  K with step of  $10^6$  K, and the range of surface gravity  $15.0 \geq \log g \geq \log g_{cr}$  (cgs units) with step of 0.1. Here we introduced the critical gravity  $g_{cr}$ , for which acceleration exerted by the radiation pressure gradient and directed outward just balances gravity. Finally, we transformed numerical ASCII models to FITS format required by the XSPEC package.

Properties of neutron star theoretical spectra were extensively discussed e.g. in Majczyna et al. (2005), see also earlier theoretical papers of this series. As an example, Fig.1 presents a model spectrum with parameters similar to these of MXB 1728-34, see Section 6 (solid line). The relevant effective temperature equals to

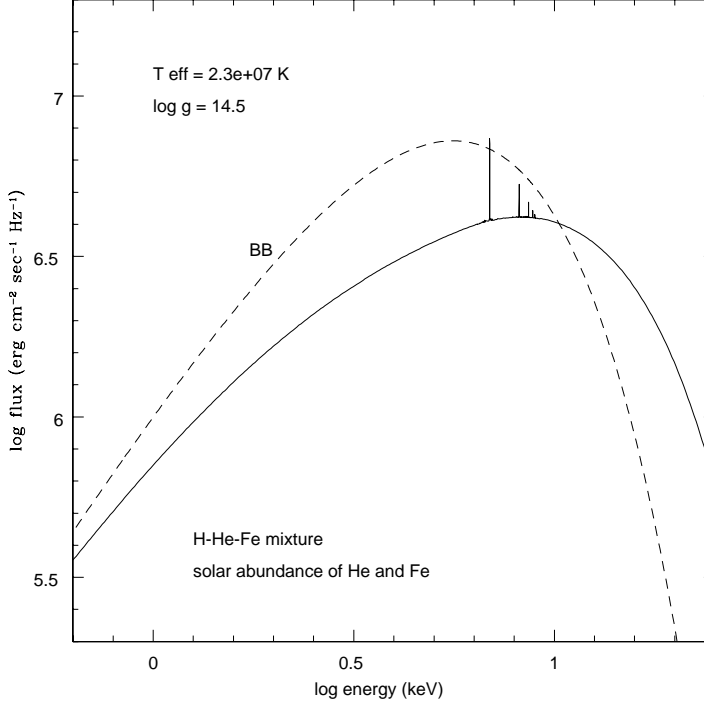


Figure 1: Comparison of the neutron star theoretical spectrum (solid line) and the blackbody spectrum (dashed line). Sample effective temperature  $T_{\text{eff}}$ , surface gravity  $\log g$  and chemical composition correspond to one of the best fits. The BB spectrum in this Figure was computed for the temperature  $T_{\text{eff}}$ .

$T_{\text{eff}} = 2.3 \times 10^7$  K, surface gravity  $\log g = 14.5$  (cgs), and chemical composition is H-He-Fe of solar proportions. Fig.1 includes also properly normalized blackbody spectrum of the temperature  $T = T_{\text{eff}} = 2.3 \times 10^7$  K. Spectrum of blackbody was routinely used in many earlier papers for the rough representation of an X-ray burst spectrum.

Fig. 1 demonstrates basic properties of our model spectrum. First, the latter is shifted to higher energies as compared with the blackbody. Such a shift is typical for scattering atmospheres (Madej 1974) and causes that the ratio of color to effective temperatures,  $T_{\text{col}}/T_{\text{eff}} > 1$ . Second, one can note that the shape of precisely computed spectrum is different than the blackbody and exhibits low energy excess and several spectral lines. In this Figure spectral lines are caused by hydrogenic iron and appear in emission.

Both the specific shape of an exact spectrum and its shift toward higher energy depend on  $T_{\text{eff}}$ ,  $\log g$  and also the redshift  $z$ . Therefore, these parameters can be determined by comparing of theoretical and observed RXTE spectra. While RXTE spectral resolution does not allow to resolve most of spectral lines, they contribute to theoretical counts in channels of RXTE proportional counters.

### 3. Observations and data analysis

X-ray burster MXB 1728-34 was observed by the RXTE satellite many times at the time period 1996-1999. In our paper we have reanalyzed archival RXTE spectral observations taken from the HEASARC database, numbered 10073-01-02-00, 10073-01-03-000, 20083-01-01-01, 20083-01-02-01, 20083-01-04-00, 20083-01-04-01. We have selected spectra obtained by the PCA instrument, since it was sensitive in the energy band 2-60 keV, and have chosen data from the top layer of detectors Pcu0, 1, 2. The above spectra correspond to the quiescent phase of the burster.

Standard-2 configuration was used to analyze the spectra. This type of configuration has a very good energy resolution, however, it has poor time resolution. We integrated raw spectra over 96 second intervals, taking shorter spectra binned to 16-sec at the time of their extraction. We selected spectra of this source outside bursts, because wanted to avoid possible phases of radius expansion of the neutron star (NS), and rapid changes of its luminosity. We did not include correction for dead time. In our case, count rate was not large and neglecting this correction generated error lower than 1%.

During preparation of an observed spectrum for fitting we neglected counts in channels below 3.0 keV, since one can expect poor energy resolution in low energy channels and too strong impact of interstellar absorption. Data above 20 keV were ignored due to poor statistics of counts. We extensively used the publicly available software XSPEC v. 11.1 and the response matrix v. 10.1. The XSPEC software was described in Arnaud (1996).

Claret et al. (1994) have discovered a hard energy excess of this source in the 30–200 keV energy band with the SIGMA telescope on board GRANAT satellite. Authors fitted hard X-ray spectrum of MXB 1728-34 by a thermal bremsstrahlung model with a very high electron temperature of  $38 \text{ keV} = 4.4 \times 10^8 \text{ K}$ . Authors did not explain what is the origin of this extremely hot medium. The existence of very hot electrons there was not confirmed at a later time.

RXTE observed the source MXB 1728-34 for a very long accumulated time period, and therefore recorded many hard X-ray photons. As was written above, we integrated our spectra over relatively short time period. For such integration time hard part of the spectrum is very weak. For example, in our template spectrum described by the number 24000 the maximum of flux exhibits about 160 counts/s/keV, and above 20 keV flux drops below 2 counts/s/keV. For such a low flux it is impossible to obtain a signal to noise ratio which is useful for fitting of any emission models. We also did not attempt to fit hard X-ray part of the spectrum since our model atmospheres are dark above 20 keV. Therefore, analyzing of hard X-ray spectrum for MXB 1728-34 with our model spectra would not yield any informations regarding  $T_{\text{eff}}$ ,  $\log g$  and the redshift  $z$ .

Characteristic features of our spectra are: line-like absorption feature around 4.5 keV and flux excess around 6.5 keV. We note the existence of such an excess in each analyzed spectrum but sometimes this feature is not prominent. Line-like feature appears in some of spectra, but sometimes it decreases to the apparent noise level. Interpretation of this feature is not clear, and fitting a model gaussian line of central energy 4.5 keV do not improve the fit. Therefore we do not attempt to model this line. What is important, the line appears only when we use the response matrix

version 1996, and in later versions of the response matrix this problem was solved. This line can be interpreted as the instrumental xenon L-edge line.

Situation is quite different in case of the flux excess around 6.5 keV. Approximating of this excess as a broad gaussian line seems necessary. PCA data did not allow us for the physically meaningful interpretation of this “line”. Also determination of the centroid energy corresponding to this line is impossible using the fitting procedure. In case of spectra recorded by other instruments like MECS on board BeppoSAX satellite such a flux excess was interpreted as the fluorescent iron line produced in cold disk illuminated by hard X-ray photons (see Di Salvo et al. 2000). Our model atmosphere do not include processes which produced  $\text{Fe} K_{\alpha}$  line, and we appended this line “by hand” using the XSPEC model of a gaussian line.

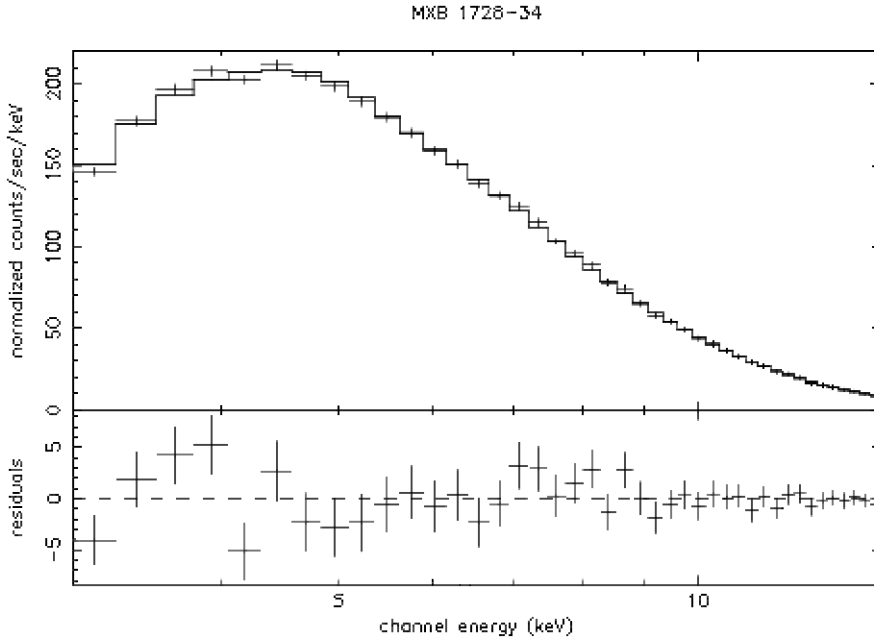


Figure 2: Sample fit of the MXB 1728-34 spectrum of 96-sec length, ObsID 10073-01-03-000. We have fitted `wabs*plabs(ATM+gaussian)` template spectra. Fit is reasonable ( $\chi^2 = 0.812$ ), and the lower panel exhibits residua.

If we restricted our analysis and used the standard template spectra of the XSPEC software, than the best fits consist of a blackbody spectrum plus power law component with high energy cutoff modified by interstellar absorption of cold matter. Moreover, if we included multicolor disk blackbody model then the best fit yields unrealistic high temperatures in the inner ring of the disk equal to 2.8 keV. Therefore, we replaced the above model by the emission from the comptonised neutron star atmosphere, corrected for low energy absorption and a gaussian line. In our solution emission from the accretion disk is assumed as negligibly small. X-ray burster MXB 1728-34 exhibits frequent bursts, with average time intervals of 8.4 hours (Basinska et al. 1984). Therefore, its atmosphere does not cool down ef-

ficiently between bursts and then X-rays from the colder disk do not contribute significantly.

We performed fitting of 18 spectra from the RXTE archive using extensive grids of theoretical spectra computed by the code ATM21, The code was described in detail e.g. in Madej (1991a); Madej, Joss & Różańska (2004); Majczyna et al. (2005), see also the previous Section.

In order to determine the effective temperature, redshift and surface gravity of the neutron star we fitted observed spectra of MXB 1728-34 with the model `wabs*plabs(ATM21+gaussian)`. Such a fitting formula denote the sum of our theoretical spectrum plus gaussian line modified by interstellar absorption and absorption caused by dust. Addition of absorption on dust is reasonable, because this burster is located in the direction to the Galactic Center, where such type of extinction is very high.

#### 4. Calculations of mass and radius

Mass and radius of the neutron star was determined from the values of surface gravity  $\log g$  and gravitational redshift  $z$ . The effective temperature  $T_{\text{eff}}$  was not useful at this step. Gravitational redshift is given by:

$$1 + z = \left(1 - \frac{2GM}{Rc^2}\right)^{-1/2} \quad (2)$$

where  $G$  is the gravitational constant,  $M$  is the neutron star mass,  $R$  is the radius measured on the NS surface,  $c$  denotes the speed of light. Gravitational acceleration on the NS surface equals to :

$$g = \frac{GM}{R^2} \left(1 - \frac{2GM}{Rc^2}\right)^{-1/2} \quad (3)$$

We solve Eqs. 1-2 for mass  $M$  and radius  $R$ , and obtain the explicit expressions:

$$R = \frac{zc^2}{2g} \frac{(2+z)}{(1+z)} \quad (4)$$

$$M = \frac{z^2 c^4}{4gG} \frac{(2+z)^2}{(1+z)^3} \quad (5)$$

Both mass and radius of a neutron star are functions only of the surface gravity  $g$  and the gravitational redshift  $z$ . The effective temperature  $T_{\text{eff}}$  (which is equivalent to the bolometric luminosity of an unit area on the NS surface) does not directly influence neither  $M$  nor  $R$ .

Moreover, our method of  $M$  and  $R$  determination for a neutron star exhibits two interesting properties:

**1.** Values of both mass and radius are independent on the distance to the source. We also do not need to estimate and compare both the bolometric and apparent X-ray luminosities of a neutron star to obtain  $M$  and  $R$ .

**2.** Both mass and radius of a NS do not depend on the estimate of the dimensionless parameter  $\xi$ , which is defined as the relative area of the NS star surface actually emitting X-rays. Our method allows one to measure  $M$  and  $R$  also in cases, when only part of the surface (of unknown value  $\xi$ ) is visible in X-rays.

#### 4.1. The minimum mass of a neutron star

For the proper determination of surface gravities and gravitational redshifts it is necessary to estimate physically reliable minimum mass for neutron stars (see Section 6). We turn attention of the reader to the paper by Haensel et al. (2002), who investigated the equation of state for dense matter and the minimum mass of neutron stars.

Haensel et al. (2002) predicted that minimum masses of cold nonrotating neutron stars are of the order  $M_{\min} \approx 0.09M_{\odot}$ , and this value depends very weakly on the equation of state. If a neutron star rotates, than the minimum mass  $M_{\min}$  increases. Haensel et al. (2002) present the example that in the case of the most rapidly rotating radio pulsar ( $P_{\text{rot}} = 1.56$  ms or frequency 641 Hz) the minimum mass of uniformly rotating cold neutron star is in the range  $0.54 - 0.61M_{\odot}$  depending on the exact equation of state.

Constraining of a NS mass was necessary to eliminate many of the fits which we deem as physically unrealistic, since they could imply low NS masses even below  $M_{\min}$ . If this constraint was not introduced, then the averaged NS masses in MXB 1728-34 would lower than these claimed in Section 7 of our paper.

## 5. Fitting procedure

We have chosen total of 18 spectra from 6 different exposures of RXTE, which correspond either to the island or banana states. We proceeded in the following way. For each model atmosphere of a given effective temperature  $T_{\text{eff}}$  (on the NS surface), logarithm of surface gravity  $\log g$ , and some trial chemical composition (see the listing in Sec. 2), we have fixed parameters of the line: central energy  $E_{\text{line}} = 6.2$  keV, and the width  $\sigma = 1.2$  keV. Redshift  $z$  was also fixed at some value in the range  $0.00 - 0.60$ . At the time of fitting we iterated the following free parameters: hydrogen column density, two parameters of the `plabs` model, normalization of the ATM21 model, and the normalization of the line (total 5 free parameters).

We iterated the above five free parameters until the minimum of  $\chi^2$  has been achieved. Such a procedure was repeated for all other combinations of  $T_{\text{eff}}$ ,  $\log g$  and  $z$ , and for all three available chemical composition. Trial values of the gravitational redshift  $z$  were changed from 0.00 to 0.60 with steps of 0.01.

The actual fitting was restricted to the effective temperatures  $T_{\text{eff}}$  in the range from  $1 \times 10^7$  K to  $3 \times 10^7$  K, changing with step of  $10^6$  K. In such a way we have obtained the table of more than 21 000 values of  $\chi^2$ , each of them corresponding to the unique set of the three fixed parameters:  $T_{\text{eff}}$ ,  $\log g$ , and  $z$ , for a given chemical composition. Then, we searched for the minimum of  $\chi^2$  in the three-dimensional space.

Inspection of the table of  $\chi^2$  showed, that the best fitted models with iron abundance 100 times greater than the solar value produced significantly higher  $\chi^2$  at numerous minima, than those obtained for hydrogen-helium models. We believe that iron rich models do not represent relevant chemical composition of the neutron star surface in quiescent state of MXB 1728-34. Therefore, fits to iron rich models will neither be presented nor discussed in subsequent Sections.

Note, that in the case of a blackbody spectrum one can determine only the quantity  $(1+z)T_{\text{eff}}$ , and the value of  $\log g$  remains unknown. Separation of  $T_{\text{eff}}$  and  $z$ ,



and the determination of  $\log g$  is possible only because shapes of real stellar spectra deviate from a blackbody. This is sometimes a marginal effect, therefore, the redshift and the surface gravity determinations can be uncertain.

## 6. Redshift and surface gravity determination

As is well known, fitting of the observed X-ray spectra with the XSPEC software usually do not produce unique results. In this research we did not obtain a unique set of  $T_{\text{eff}}$ ,  $\log g$  and  $z$ , which would have a value of  $\chi^2$  distinctly lower than remaining fits. Instead, we always obtained numerous sets of the above fitting parameters with  $\chi^2$  very close to the minimum value.

For a given chemical composition we have selected the set of  $T_{\text{eff}}$ ,  $\log g$  and  $z$  from thousands of fits which corresponds to the minimum value,  $\chi_{\text{min}}^2$ . We have appended other sets with  $\chi^2$  in the range  $[\chi_{\text{min}}^2, \chi_{\text{min}}^2 + \Delta_1]$ , where  $\Delta_1$  represents the increase of  $\chi^2$  small enough to be in the 1-sigma confidence range.

Sizes of various confidence ranges were estimated by Avni (1976), Lampton, Margon & Bowyer (1976) and Press et al. (1996). Theoretical models fitted in this research have 5 free parameters and, typically, 38 degrees of freedom (38 d.o.f.). We applied here values for  $\Delta\chi^2$  taken from Press et al. (1996), page 692, which give in our case  $\Delta_1 = 5.89/38 \text{ d.o.f.} = 0.16$ . Such a value of  $\Delta_1$  was used in the following stages of our research.

For each of the analyzed 96 sec X-ray spectrum for MXB 1728-34 we obtained usually few hundred sets of  $T_{\text{eff}}$ ,  $\log g$  and  $z$  which belong to the  $[\chi_{\text{min}}^2, \chi_{\text{min}}^2 + \Delta_1]$  range.

Shape of the confidence levels indicate that these parameters are not correlated, see Fig. 3.

We automatically computed mass  $M$  and radius  $R$  from Eqs. 4 – 5 and rejected all sets of parameters where  $M < 0.1M_{\odot}$ . In such a way the number of acceptable fits was significantly reduced in order to secure physical reliability of fits used in further considerations.

Table 1: The best values and 1- $\sigma$  confidence ranges for  $\log g$  and  $z$

	H-He	H-He-Fe
$z_{\text{best}}$	0.14	0.22
	0.06 - 0.21	0.06 - 0.41
$\log g_{\text{best}}$	14.6	14.6
	14.2 - 14.9	14.2 - 14.9

Our determinations of the surface gravitational redshift can be compared with the value of  $z = 0.35$  given by Cottam et al. (2002) for other neutron star, EXO 0748-676.

Our determinations of the surface gravity  $\log g$  for the neutron star MXB 1728-34 are in agreement with theoretical considerations by Bejger and Haensel (2004). Both authors determined, that the maximum value of the surface gravity  $\log g =$

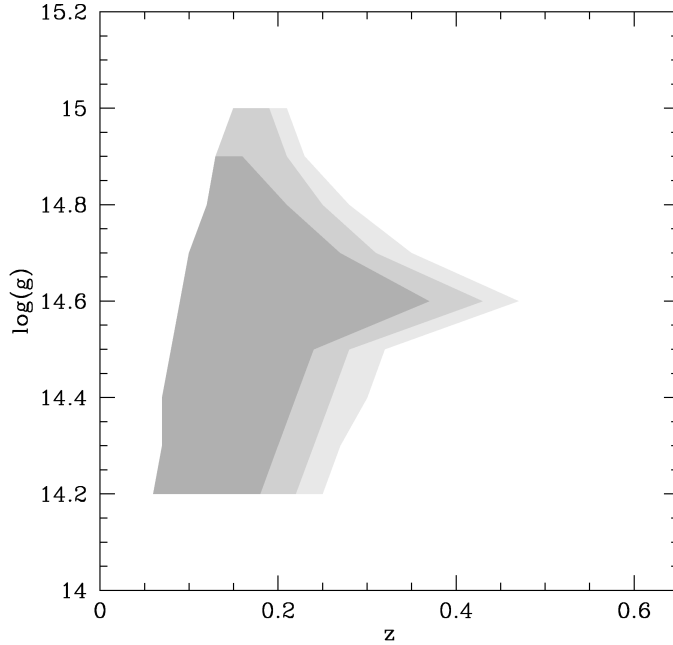


Figure 3: 1, 2, and 3-sigma confidence level for the fit of the model with solar iron abundance. Here we assume that  $M_{NS} \geq 0.1M_{\odot}$ .

14.87 for a neutron star build up of normal (hadronic) matter, and  $\log g = 14.78$  for a strange star.

## 7. Mass and radius determination

This Section presents the final results of our analysis for both assumed chemical compositions.

Our results are explained in detail in Tables 2 and 3. Each row of both Tables presents detailed analysis for each of the 96 sec spectra taken into account in this paper. Columns of both Tables give: identification of the observation, name of the spectrum, the range of  $\log g$  and  $z$  which are located in the  $1-\sigma$  confidence range, and the minimum  $\chi^2$ . The last two columns present the final results: ranges of the NS masses and radii corresponding to the  $1-\sigma$  confidence range.

In order to properly weight the averaged  $1-\sigma$  limits of investigated parameters, we have computed the arithmetic averages of the lower and upper limits for  $\log g$ ,  $z$ ,  $M$  and  $R$  in Tables 2 and 3. Results also are displayed in Tables 1 and 4 and they represent the best values of parameters for the compact star in MXB 1728-34.

The averaged values of  $M$ ,  $R$  and their  $1-\sigma$  confidence ranges are presented in Table 4.

As is evident, both mass and radius of the neutron star in MXB 1728-34 are very low as compared with canonical values. This is true for both H-He and H-He-Fe chemical compositions of a neutron star atmosphere. In any event, our  $M$  and

Table 2: Listing of archival X-ray spectra for MXB 1728-34 chosen for the  $T_{eff}$ ,  $\log, g$  and  $z$  determination with H-He model atmospheres.

Fitting of RXTE data was done with the model `wabs*plabs(ATM21+gaussian)`, where  $g$  is expressed in  $\text{cm s}^{-2}$ . The column ‘‘Spectrum’’ gives the number of seconds which elapsed between the beginning of the observation run of ID number and the beginning of the actual 96 sec time interval.

Observation ID	Spectrum	State <sup>a</sup>	$\log(g)$	$z$	$\chi^2_{\nu}$	Mass [ $M_{\odot}$ ]	Radius [km]
10073-01-02-00	2244	IS	14.1 – 14.9	0.05 – 0.24	0.846	0.1 – 0.8	1.4 – 8.9
	13072	IS	14.2 – 14.9	0.06 – 0.20	0.770	0.1 – 0.6	1.4 – 7.5
10073-01-03-000	768	IS	14.2 – 14.9	0.06 – 0.23	0.815	0.1 – 0.7	1.4 – 8.4
	11904	IS	14.2 – 14.9	0.06 – 0.24	0.825	0.1 – 0.8	1.4 – 8.9
	13152	IS	14.2 – 14.9	0.06 – 0.21	0.808	0.1 – 0.7	1.4 – 8.0
20083-01-01-01	7392	UB	14.2 – 15.0	0.07 – 0.24	0.854	0.1 – 0.9	1.3 – 8.9
	7584	UB	14.1 – 15.0	0.05 – 0.25	0.938	0.1 – 0.9	1.3 – 9.4
20083-01-02-01	500	UB	14.6 – 14.9	0.09 – 0.15	0.720	0.1 – 0.3	1.4 – 3.2
	700	UB	14.1 – 15.0	0.05 – 0.28	0.628	0.1 – 1.3	1.3 – 11.4
	1000	UB	14.1 – 15.0	0.05 – 0.25	0.906	0.1 – 1.0	1.3 – 9.9
	1200	UB	14.6 – 14.9	0.10 – 0.17	0.850	0.1 – 0.3	1.4 – 3.4
	2000	UB	14.2 – 15.0	0.07 – 0.24	0.750	0.1 – 0.9	1.3 – 9.4
20083-01-04-00	6000	UB	14.1 – 14.9	0.05 – 0.24	0.938	0.1 – 0.9	1.4 – 9.4
	1500	LB	14.2 – 14.9	0.06 – 0.20	0.576	0.1 – 0.6	1.4 – 7.5
	7300	LB	14.2 – 14.9	0.06 – 0.23	0.897	0.1 – 0.7	1.4 – 8.5
	12240	LB	14.2 – 14.9	0.06 – 0.23	0.845	0.1 – 0.8	1.4 – 8.9
20083-01-04-01	24000	LB	14.2 – 14.6	0.06 – 0.14	0.754	0.1 – 0.3	1.9 – 4.4
	24900	LB	14.4 – 14.5	0.07 – 0.10	0.915	0.1 – 0.2	2.2 – 3.1

<sup>a</sup> Spectral states: IS – island state, UB – upper banana state, LB – lower banana state.

$R$  determinations are consistent with a family of currently known equations of state for superdense matter. Our best values of mass  $M$  and radius  $R$  clearly suggest, that the neutron star in MXB 1728-34 is composed of strange matter (see Figs. 4-5).

Results presented in Tables 1 – 4 clearly suggest, that the canonical mass of  $1.4 M_{\odot}$  is rather excluded by almost all of our detailed fits, no matter what is the exact chemical composition of model atmospheres among the two presented in this paper. There exists only a single 96 s spectrum in Table 3 which contradicts this statement, however, that fit is not really good because the redshift  $z$  is very poorly constrained. Therefore, it yields rather indefinite results on both the mass  $M$  and radius  $R$ .

The radius  $R = 10 – 12$  km is thought to represent the canonical value. Tables 1 and 4 show that these values are on the fringe of our  $1-\sigma$  confidence range. In other words, centroids of fits in Figs. 1 – 4 show that the neutron star in MXB 1728-34 is much smaller and less massive than the canonical NS star.

Note, that masses  $M$  and radii  $R$  determined in this paper are partially correlated, as is shown in Figs. 3 – 4. This means, that the area on the  $M \times R$  plane which is permitted by our determinations is much smaller than the area of the rectangle of the size given by the confidence ranges from Table 4.

The above results strongly suggest, that the ‘‘neutron’’ star in MXB 1728-34 is

Table 3: The same for fits to the grid of model atmospheres with solar iron abundance.

Observation ID	Spectrum	State	log(g)	z	$\chi^2_{\nu}$	Mass [ $M_{\odot}$ ]	Radius [km]
10073-01-02-00	2244	IS	14.2 – 14.9	0.06 – 0.37	0.848	0.1 – 1.1	1.4 – 9.4
	13072	IS	14.2 – 14.8	0.06 – 0.30	0.772	0.1 – 0.8	1.6 – 6.4
10073-01-03-000	768	IS	14.2 – 14.9	0.06 – 0.34	0.814	0.1 – 1.0	1.4 – 8.5
	11904	IS	14.2 – 14.9	0.06 – 0.30	0.805	0.1 – 0.8	1.4 – 8.0
	13152	IS	14.2 – 14.8	0.06 – 0.34	0.833	0.1 – 1.0	1.6 – 8.0
20083-01-01-01	7392	UB	14.2 – 15.0	0.06 – 0.44	0.885	0.1 – 1.5	1.3 – 11.4
	7584	UB	14.2 – 15.0	0.06 – 0.38	0.836	0.1 – 1.2	1.3 – 9.4
20083-01-02-01	500	UB	14.2 – 14.9	0.06 – 0.39	0.997	0.1 – 1.2	1.4 – 8.9
	700	UB	14.2 – 15.0	0.06 – 0.49	0.569	0.1 – 2.0	1.3 – 14.6
	1000	UB	14.2 – 15.0	0.06 – 0.45	0.968	0.1 – 1.5	1.3 – 11.8
	1200	UB	14.2 – 15.0	0.06 – 0.42	1.000	0.1 – 1.4	1.3 – 10.4
	2000	UB	14.2 – 15.0	0.06 – 0.44	0.729	0.1 – 1.5	1.3 – 11.8
	6000	UB	14.2 – 15.0	0.06 – 0.43	0.993	0.1 – 1.4	1.3 – 10.9
20083-01-04-00	1500	LB	14.2 – 14.9	0.06 – 0.38	0.552	0.1 – 1.2	1.4 – 8.9
	7300	LB	14.2 – 14.8	0.06 – 0.34	0.932	0.1 – 1.0	1.6 – 6.7
	12240	LB	14.2 – 14.9	0.06 – 0.39	0.843	0.1 – 1.2	1.4 – 9.4
	24000	LB	14.2 – 15.0	0.06 – 0.34	0.769	0.1 – 1.0	1.6 – 6.7
20083-01-04-01	24900	LB	14.6 – 14.6	0.09 – 0.16	0.985	0.1 – 0.3	1.9 – 3.4

Table 4: The best values and 1- $\sigma$  confidence ranges for  $M$  and  $R$

	H-He	H-He-Fe
$M_{\text{best}} [M_{\odot}]$	0.40	0.63
	0.1 - 0.7	0.1 - 1.2
$R_{\text{best}} [\text{km}]$	4.58	5.27
	1.4 - 7.7	1.4 - 9.1

composed of strange matter, see Figs. 3 – 4. We cannot exclude, however, that the NS star in this object is build up of normal matter if we investigate the 1- $\sigma$  confidence range for both  $M$  and  $R$ .

## 8. Comments

Few additional comments can be appended to our method and results, which were presented in the previous Section.

1. First, one can immediately determine the compactness of the MXB 1728-34, which is the ratio of mass (in solar masses) to radius (in km), see Nath et al. (2002). We find that the compactness  $M/R$  of the MXB 1728-34 source obtained in this paper equals to 0.087 (H-He models), or 0.12 for H-He-Fe models.

Nath et al. (2002) discovered millisecond X-ray oscillations in the rising part of light curves in two bursts of this source. Observations were performed by RXTE in

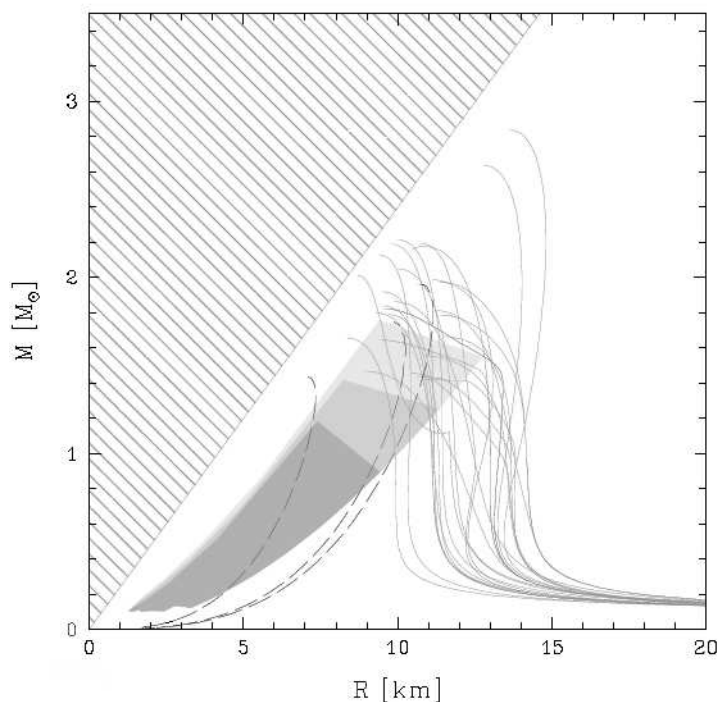


**Figure 4:** Position of MXB 1728-34 on the  $M - R$  diagram determined from models with iron in solar proportion. We adapted Fig. 2 from Bejger and Haensel (2002), who plotted here examples of 30 equations of state for quark matter (dashed lines), and normal matter or normal matter plus strange matter (solid lines). The shaded area is excluded by General Relativity and causality condition. Our determinations for the  $M$  and  $R$  confidence ranges are shown by gray contours: dark gray area is the  $1-\sigma$  confidence level, medium –  $2-\sigma$  and light gray area –  $3-\sigma$  confidence level.

1996-1997, and these X-ray oscillations were subsequently fitted by radiation from either one or two hot spots on the surface of a rotating neutron star. Taking into account the relativistic deflection of emitted X-rays, they found the averaged value of  $M/R = 0.121$  for MXB 1728-34. Our determinations of the  $M/R$  are consistent with their findings.

2. Recently Shaposhnikov and Titarchuk (2002) have published numerical model for the computation of the structure of a neutron star atmosphere and its X-ray spectrum for the expansion stage of X-ray burst. I.e. their model is applicable to the phase when radiation forces approach gravitational forces. On the contrary, we used model atmospheres in hydrostatic equilibrium, therefore, our theoretical X-ray spectra represent spectra of a neutron star with the luminosity significantly lower than the Eddington luminosity (quiescent state).

Note, that Shaposhnikov and Titarchuk (2002) followed the strategy in which their model spectra were approximated by a blackbody spectrum, where possible. We have followed opposite strategy. Our theoretical X-ray spectra of neutron star were never approximated by some models. In this way we made use of even slight

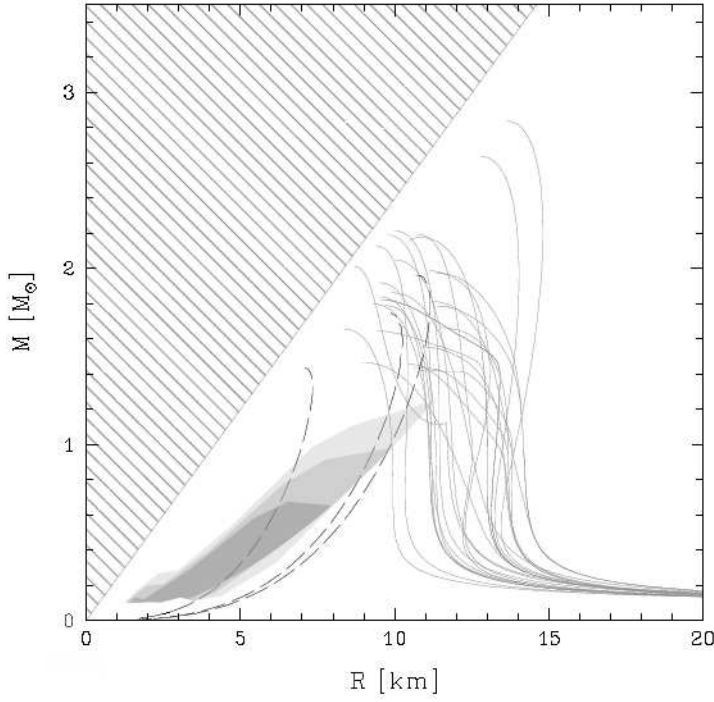


Figure 5: Position of MXB 1728-34 on the  $M - R$  diagram determined from models containing hydrogen and helium in solar proportion. We adapted Fig. 2 from Bejger and Haensel (2002), who plotted here examples of 30 equations of state for quark matter (dashed lines), and normal matter or normal matter plus strange matter (solid lines). The shaded area is excluded by General Relativity and causality condition. Our determinations of the NS confidence ranges of the parameters are denoted by gray areas: dark gray area is the  $1-\sigma$  confidence level, medium –  $2-\sigma$  and light gray area –  $3-\sigma$  confidence level.

deformations of theoretical continuum spectra as compared with the blackbody, and discrete spectral features of iron to fit X-ray observations and extract as much informations about a neutron star as possible (i.e. values of redshift  $z$  and  $\log g$  simultaneously).

**3.** We stress here, that all our determinations of parameters for MXB 1728-34 were obtained assuming the particular model for fitting, `wabs*plabs(ATM21+gaussian)`. We have chosen this model also because it produced reasonably low  $\chi^2$  for the best fits. In future we plan to seek also for other models for the same set of X-ray spectra of MXB 1728-34, as these in Tables 2 and 3.

## 9. Summary

We present in this paper the determination of mass, radius, surface gravity and the gravitational redshift for the neutron star in X-ray burster MXB 1728-34. For the first time such results were obtained by fitting of archival RXTE raw spectra

of this source in quiescent state to grids of advanced models of hot neutron star theoretical X-ray spectra. The latter were computed with the ATM21 code which was extensively described e.g. in Madej (1991a), Madej et al. (2004), and Majczyna et al. (2005).

We have fitted 18 of 96-sec RXTE spectra to three available grids of hot NS theoretical spectra, corresponding to different chemical composition of models. Two grids of models yielded very good fits: the hydrogen-helium model atmospheres with solar He abundance (hereafter the grid 1), and the H-He-Fe grid with solar iron abundance hereafter the grid 2). We ruled out the grid of H-He-Fe mixture with iron abundance 100 times the solar value, since it always yielded much worse  $\chi^2$  values than the first two chemical compositions.

Both the former chemical compositions ensure fits of similar credibility. We conclude that the best determined parameters of the neutron star in MXB 1728-34 are: the surface gravity is  $\log g = 14.6$  (grid 1) or  $14.6$  (grid 2), and the surface redshift  $z = 0.14$  (1) or  $0.22$  (2). There are, however, rather large sizes of  $1-\sigma$  confidence ranges, particularly for the surface redshift  $z$ , see Section 6. These parameters imply low values of mass  $M$  and radius  $R$  of the neutron star: mass  $M = 0.40M_{\odot}$  (1) or  $0.63M_{\odot}$  (2), and the radius  $R = 4.58$  km (1) or  $5.27$  km (2).

Note, that these results were obtained assuming the particular model for fitting, `wabs*plabs (ATM+gaussian)`.

Our method of the surface gravity, gravitational redshift, mass and radius determination for a neutron star takes into account the shape of a NS continuum X-ray spectrum and its location on the energy-flux diagram. The method does not make any reference to the (poorly known) distance to the source and its bolometric or Eddington luminosities. Our method of the determination of the above four (global) parameters of the NS does not make any reference to the question whether the whole surface of the NS or only part of it is visible in X-ray satellite detectors.

Our results imply that the NS star in MXB 1728-34 in fact is composed of strange matter, see Figs. 3 and 4. Therefore, we confirm the hypothesis proposed by Li et al. (1999), who noted that the M-R relation for MXB 1728-34 is typical for the equation of state of strange matter. Of course, a bare quark star can not be the source of bursts. However, a quark star with a crust and external envelope composed of normal matter can exhibit bursts (Miralda-Escudé et al. 1990).

**Acknowledgements.** We thank Michał Bejger, Paweł Haensel, Mirosław Należyty and Ewa Szuszkiewicz for their helpful comments regarding our research on MXB 1728-34. This work has been supported by the Polish Committee for Scientific Research grant No. 1 P03D 001 26.

This research has made use of data obtained from the High Energy Astrophysics Science Archive Research Center (HEASARC), provided by NASA's Goddard Space Flight Center.

## REFERENCES

- Arnaud K.A. 1996, in *Astronomical Data Analysis Software and Systems*, V ASP Conf. Ser., 101. 17 (eds. G.H. Jacoby and J. Barnes)  
 Avni Y. 1976, *Astrophys. J.*, **210**, 642.

- Basinska E.M., Lewin, W.H.G., Sztajno, M., Cominsky, L.R., and Marshall, F.J. 1984, *Astrophys. J.*, **281**, 337.
- Bejger M. and Haensel P. 2002, *A&A*, **396**, 917.
- Bejger M. and Haensel P. 2004, *A&A*, **420**, 987.
- Cottam, J., Paerels, F. and Mendez, M. 2002, *Nature*, **420**, 51.
- Claret A., Goldwurm, A., Cordier, B. et al. 1994, *Astrophys. J.*, **423**, 436.
- Di Salvo T., Iaria, R., Burderi, L., and Robra, N.R. 2000, *Astrophys. J.*, **542**, 1034.
- Forman W., Tananbaum H. and Jones C. 1976, *Astrophys. J.*, **206**, L29.
- Foster, A.J., Ross, R.R., Fabian, A.C. 1986, *MNRAS*, **221**, 409.
- Galloway D.K., Psaltis, D., Chakrabarty, D., and Muno, M.P. 2003, *Astrophys. J.*, **590**, 999.
- Guilbert, P.W. 1981, *MNRAS*, **197**, 451.
- Haensel P., Zdunik J.L. and Douchin F, 2002, *A&A*, **385**, 301.
- Joss, P.C. & Madej, J. 2001, *Two Years of Science with Chandra*, , Washington, DC, 5-7 September, 2001.
- Kaminker A.D., Pavlov, G.G., Shibanov, Y.A., Kurt, V.G., Smirnov, A.S., Shamolin, V.M., Kopaeva, I.F., and Sheffer, E.K. 1989, *A&A*, **220**, 117.
- Lampton M., Margon B. & Bowyer S. 1976, *Astrophys. J.*, **208**, 177.
- Margon B., Lampton M. Bowyer S., Cruddace R. 1975, *Astrophys. J.*, **197**, 25.
- Lewin W.H.G., Clark G., and Doty J. 1976, *IAU Circ.*, **2922**, .
- Li X.-D., Ray, S., Dey, J., Dey, M., and Bombaci, I. 1999, *Astrophys. J.*, **527**, L51.
- Madej J. 1974, *Acta Astron.*, **24**, 327.
- Madej J. 1991a, *Astrophys. J.*, **376**, 161.
- Madej J. 1991b, *Acta Astron.*, **41**, 73.
- Madej J., Joss P.C., and Róžańska A. 2004, *Astrophys. J.*, **602**, 904.
- Majczyna, A., Madej, J., Joss, P.C., Róžańska, A. 2002, *High Resolution X-ray Spectroscopy with XMM-Newton and Chandra*, 0 Mullard Space Science Lab., University College London, U.K., 24-25 October, **2002**, p. E23.
- Majczyna, A., Madej, J., Joss, P.C. and Róžańska, A. 2005, *A&A*, **430**, 643.
- Martí J., Mirabel, I.F., Rodríguez, L.F., and Chaty, S. 1998, *A&A*, **332**, L45.
- Mihalas, D. 1978, *Stellar Atmospheres*, W.H. Freeman & Co., San Francisco, . .
- Miralda-Escudé J., Haensel P., Paczyński B. 1990, *Astrophys. J.*, **362**, 572.
- Nath, N.R., Strohmayer, T.E., Swank, J.H. 2002, *Astrophys. J.*, **564**, 353.
- Osheroich V. & Titarchuk L. 1999, *Astrophys. J.*, **522**, L113.
- Press W.H., Vetterling W.T., Teukolsky S.A., Flannery B.P. 1996, "Numerical Recipes. Second Edition." (Cambrige Univ. Press), . .
- Shaposhnikov, N. & Titarchuk, L. 2002, *Astrophys. J.*, **567**, 1077.
- Shaposhnikov, N., Titarchuk, L. & Haberl, F. 2003, *Astrophys. J.*, **593**, L35.
- Strohmayer T.E., Zhang W., Swank J.H. 1997, *Astrophys. J.*, **487**, L77.
- Titarchuk L. 1994, *Astrophys. J.*, **434**, 570.
- Titarchuk L. & Osheroich V. 1999, *Astrophys. J.*, **518**, L95.
- Titarchuk L. & Shaposhnikov N. 2002, *Astrophys. J.*, **570**, L25.
- van Paradijs, J. 1978, *Nature*, **274**, 650.
- van Paradijs, J. 1979, *ApJ*, **234**, 609.